



# On the classical and fractional control of a nonlinear inverted cart-pendulum system: a comparative analysis

José Geraldo Telles Ribeiro, Julio Cesar de Castro Basilio, Americo Cunha Jr,  
Tiago Roux Oliveira

## ► To cite this version:

José Geraldo Telles Ribeiro, Julio Cesar de Castro Basilio, Americo Cunha Jr, Tiago Roux Oliveira.  
On the classical and fractional control of a nonlinear inverted cart-pendulum system: a comparative analysis. José Manoel Balthazar. Vibration Engineering and Technology of Machinery, Springer, Cham, pp.397-417, 2021, 10.1007/978-3-030-60694-7\_26 . hal-02682328

HAL Id: hal-02682328

<https://hal.archives-ouvertes.fr/hal-02682328>

Submitted on 1 Jun 2020

**HAL** is a multi-disciplinary open access archive for the deposit and dissemination of scientific research documents, whether they are published or not. The documents may come from teaching and research institutions in France or abroad, or from public or private research centers.

Copyright

L'archive ouverte pluridisciplinaire **HAL**, est destinée au dépôt et à la diffusion de documents scientifiques de niveau recherche, publiés ou non, émanant des établissements d'enseignement et de recherche français ou étrangers, des laboratoires publics ou privés.

# **On the classical and fractional control of a nonlinear inverted cart-pendulum system: a comparative analysis**

**José Geraldo Telles Ribeiro<sup>1</sup>, Julio Cesar de Castro Basilio<sup>2</sup>,  
Americo Cunha Jr<sup>3</sup>, Tiago Roux Oliveira<sup>4</sup>**

<sup>1</sup>Rio de Janeiro State University - UERJ, Department of Mechanical Engineering  
jose.ribeiro@uerj.br

<sup>2</sup>Rio de Janeiro State University - UERJ, Department of Mechanical Engineering  
basilio.julio@posgraduacao.uerj.br

<sup>3</sup>Rio de Janeiro State University - UERJ, Department of Applied Mathematics  
americoo@ime.uerj.br

<sup>4</sup>Rio de Janeiro State University - UERJ, Department of Electronics and Telecommunication Engineering  
tiagoroux@uerj.br

**Abstract.** The use of fractional-order controllers to drive dynamical systems to a desired/target configuration became extremely popular in the last decade, with many studies stating that they present superior performance when compared to the integer-order counterparts, especially for nonlinear systems. Following this trend, the purpose of this chapter is to verify the possibility of improving the performance of the control of an inverted cart-pendulum system using fractional-order integrators. The strategy is to employ the classical pole location linear method to calculate the gains of the controller and then to compare the performance between integer-order and fractional-order integrators, the last one that are calculated using an optimization method.

**Keywords:** fractional calculus, state-derivative feedback, fractional-order control, cart-pendulum nonlinear system

## **1 Introduction**

The idea of the Fractional Calculus was introduced in 1695 when Bernoulli, Leibniz, and L'Hôpital exchanged letters about the possibility of a non-integer derivative order. This discussion involved many mathematicians as Euler, Fourier, and Laplace, among others (Monje et al. 2010; Ortigueira 2011; Ortigueira

and Manuel 2015). During the following centuries, many pure and applied mathematicians contributed to the development of the fractional calculus theory and many different fractional operators have been proposed, among them the Grünwald-Letnikov, Riemann-Liouville and Caputo fractional derivatives (Li and Dend, 2007).

The Riemann-Liouville fractional integral (Li and Deng 2007) of order  $\alpha$ , where  $\alpha \in \mathbb{R}$  and  $\alpha > 0$ , is defined in terms of a convolution type operation between the real-valued function  $y(t)$  and the kernel  $t^{\alpha-1}$

$$I_{a,t}^\alpha y(t) = \frac{1}{\Gamma(\alpha)} \int_a^t (t-\tau)^{\alpha-1} y(\tau) d\tau , \quad t > a \quad (1)$$

being  $\Gamma$  the Gamma function, and the Riemann-Liouville fractional derivative (Li and Dend, 2007) is defined in terms of the classical derivative of order  $n \in \mathbb{Z}^+$  of this fractional-order integral

$${}_{RL}D_{a,t}^\alpha y(t) = \frac{1}{\Gamma(n-\alpha)} \frac{d^n}{dx^n} \int_a^t (t-\tau)^{n-\alpha-1} y(\tau) d\tau \quad (2)$$

$$t > a, \quad n-1 < \alpha < n,$$

which is a global operator (not local as in classical calculus) that presents “memory”.

However, other definitions for a fractional derivative are also possible, like one by Grünwald-Letnikov (Li and Deng 2007)

$${}_{GL}D_{a,t}^\alpha y(t) = \lim_{N \rightarrow \infty} \left\{ \frac{\left(\frac{t-a}{N}\right)^{-\alpha}}{\Gamma(-\alpha)} \sum_{j=0}^{N-1} \frac{\Gamma(j-\alpha)}{\Gamma(j+1)} y\left(t-j\left(\frac{t-a}{N}\right)\right) \right\} \quad (3)$$

$$t > a, \quad n-1 < \alpha < n,$$

or a recent definition by Caputo [4]

$${}_{C}D_{a,t}^\alpha y(t) = \frac{1}{\Gamma(n-\alpha)} \int_a^t (t-\tau)^{n-\alpha-1} y^{(n)}(\tau) d\tau \quad (4)$$

$$t > a, \quad n-1 < \alpha < n .$$

The development of new definitions is an active field of research in mathematics (Caputo and Fabrizio 2015; Khalil et al. 2014; Zheng and Zhao 2019 Ortigueira and Trujillo 1012; Katugampola 2011), but in the last decade, mainly thanks to the development of numerical methods to simulate fractional systems (Li et al. 2011; Deng et al. 2015; Tepljakov et al. 2011), fractional operators started to be used in engineering analysis (Katsikadelis 2015; Caputo and Carcione 2011; Lewandowski and Pawlak 2018; Lin et al. 2019; Dai et al. 2017) and control theory (Tepljakov 2017; Shah and Agashe 2016; Chen et al. 2018; Bingul et al. 2018; Li et al. 2016; Balachandran et al. 2015; Barbosa et al. 2010;

Wang et al. 2009 Xue and Zhao 2007; Delavari 2010), especially when dealing with time-delay (Martelli 2009) or nonlinear and chaotic systems (Azar et al. 2017; Niu 2017; Shen et al. 2014; Shen et al. 2014).

Among the favorable characteristics these fractional-order operators offer, two of them can be highlighted: (i) their global application provide a natural framework for describing phenomena with memory; and (ii) the fractional exponent offers a kind of additional degree of freedom to tune a controller, opening opportunities for additional improvements of performance in the controller design.

Trying to explore this second feature, in this manuscript a state-feedback control system is proposed to stabilize an inverted cart-pendulum system (Figure 1) and then, the possibility of improving the performance of the control system using fractional integrators is analyzed. The inverted pendulum has been chosen as a benchmark since it is a classical control problem a nonlinear system widely studied using integer-order controllers (Kharola et al. 2016; Wang et al. 2014; Prasad et al. 2014; Wang 2011), which started to be tested in fractional-control literature as well (Mousa et al. 2017).

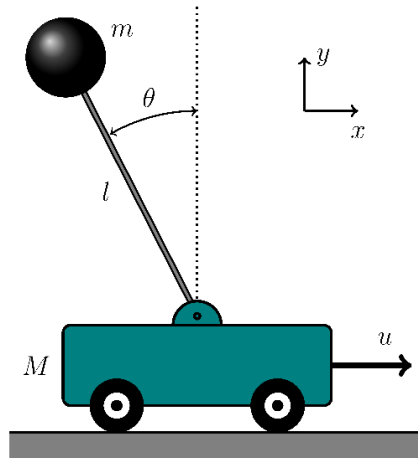


**Figure 1:** Schematic illustration of the cart-pendulum system.

## 2 Proposed control system

Figure 2 shows the state-space feedback control system proposed to control the inverted cart-pendulum system. It can be noted that the angular velocity of the pendulum and the velocity of the mass are chosen to be the observed states and they must be integrated  $I^\alpha$ , as defined by the Riemann-Liouville fractional integral in Equation 1, to obtain the angular position of the pendulum and the position of the mass, respectively.

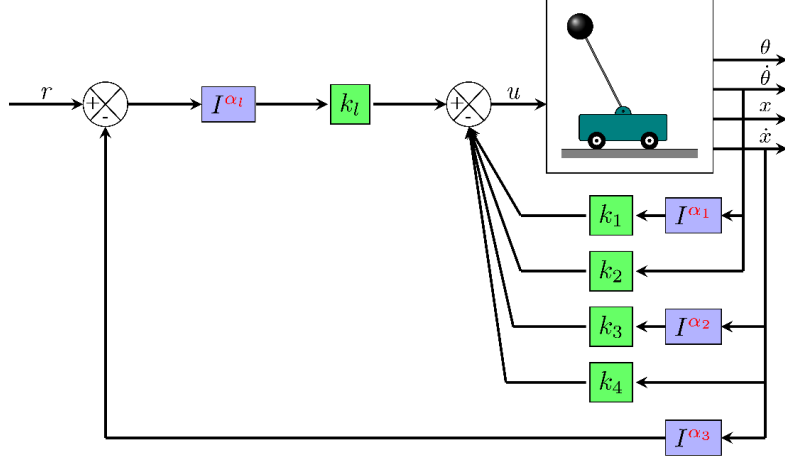


**Figure 2: Illustration of the proposed controller for the inverted cart-pendulum system.**

The pole location is a classical and widely used method used to calculate the values of each gain  $k_i$  and that has been developed for linear systems using integer-order controllers. The locations of the poles are chosen based on the performance desired for the closed-loop system. Since this method is based on linear system hypothesis, the linearized cart-pendulum model is employed

$$\begin{aligned} ml\ddot{x} + (I + ml^2)\ddot{\theta} - mgl\theta &= 0 \\ (M + m)\ddot{x} + ml\ddot{\theta} - u &= 0, \end{aligned} \tag{5}$$

where  $M$  is the cart mass;  $m$  is the inverted pendulum mass;  $I$  is pendulum moment of inertia;  $l$  is the distance from the center of pendulum's mass to the fixation point;  $\theta$  is the angle between the pendulum and a perpendicular axis through the cart's centroid;  $x$  is the cart's horizontal displacement; and  $u$  is the force applied to the cart to control the system.

Now define the state variables  $x_1, x_2, x_3$  and  $x_4$  as  $x_1 = \theta, x_2 = \dot{\theta}, x_3 = x, x_4 = \dot{x}$ . Then considering the angular position  $\theta$  and cart position  $x$  as the outputs of the system, obtained the equations for the system as follows:

$$\begin{aligned} \dot{\mathbf{x}} &= \mathbf{Ax} + \mathbf{Bu}, \\ y &= \mathbf{Cx}, \\ u &= -(k_1 I^{\alpha_1} + k_2)x_2 + (k_3 I^{\alpha_2} + k_4)x_4 + k_l \xi, \\ D^{\alpha_l} \xi &= r - y = r - I^{\alpha_3}x_4, \end{aligned} \tag{7}$$

where  $\mathbf{x}$  is the state vector;  $u$  is the control signal;  $y$  is the output signal;  $\xi$  is the output of the integrator;  $r$  is the reference input signal;  $\mathbf{A}$  is the matrix of states;  $\mathbf{B}$  is the input matrix;  $\mathbf{C}$  is the output matrix; and  $\mathbf{K}$  is the gain matrix ( $k_1, k_2, k_3$  and  $k_4$ ).

For this cart-pendulum, the matrices are:

$$\mathbf{A} = \begin{bmatrix} 0 & 1 & 0 & 0 \\ \frac{mgl(M+m)}{I(M+m)+Mml^2} & 1 & 0 & 0 \\ 0 & 0 & 0 & 1 \\ -\frac{m^2gl^2}{I(M+m)+Mml^2} & 0 & 0 & 0 \end{bmatrix}, \quad (8)$$

$$\mathbf{B} = \begin{bmatrix} 0 \\ -\frac{ml}{I(M+m)+Mml^2} \\ 0 \\ \frac{I+ml^2}{I(M+m)+Mml^2} \end{bmatrix}, \quad \mathbf{C} = [1 \ 0 \ 0 \ 0].$$

The following values are adopted for the system parameters:

$$m = 0.1 \text{ kg}, M = 2 \text{ kg}, l = 0.5 \text{ m} \text{ and } I = 0.006 \text{ kg} \cdot \text{m}^2.$$

The linear model using classical control will be used to obtain values for the  $k'$ s. It will be used the pole location method and the closed-loop poles are chosen to be located at:

$$\mu_1 = -1 + j\sqrt{3} \quad \mu_2 = -1 - j\sqrt{3} \quad \mu_3 = -5 \quad \mu_4 = -5 \quad \mu_5 = -5,$$

where  $j = \sqrt{-1}$ .

Using the Matlab to calculate the  $k'$ s, the following values are obtained:

$$k_1 = -200.6 \quad k_2 = -50.3 \quad k_3 = -70.1 \quad k_4 = -46.8 \quad k_l = -63.8.$$

The next step is to verify if the performance of the system can be improved changing the orders of the integrators by simulations using the FOMCOM toolbox (Tepljakov 2011). The simulations are done considering the following initial conditions:

$$\theta_0 = 10^\circ \quad \dot{\theta}_0 = 0 \quad x_0 = 0 \quad \dot{x}_0 = 0.$$

Since it is desired to verify the basins of attraction of the closed loop system, the simulations also consider a nonlinear model of the inverted cart-pendulum, given by

$$\begin{aligned} ml \cos \theta \ddot{x} + (I + ml^2)\ddot{\theta} - mgl \sin \theta &= 0 \\ (M + m)\ddot{x} + ml \cos \theta \ddot{\theta} - ml \sin \theta \dot{\theta}^2 - u &= 0. \end{aligned} \quad (9)$$

Another decision is to maintain the values of  $\alpha_3$  and  $\alpha_l$  equal to 1. This decision is based in the fact that lower values would introduce an offset in the mass position and higher values would make the position of the mass more oscillatory.

### 3 Fractional-controller optimization

Simulations are performed to evaluate the behavior of the control-system integrators with the combination of different orders, integer and fractional, and so find the point or region where the performance criteria are minimal.

These simulations are divided into two stages: global analysis and detailed analysis. In the first stage, the global analysis is performed observing the performance in a larger range of integrators, where the integrators had their order varied by 0.05 between:

$$0.1 \leq \alpha_1 \leq 2.0 \quad \text{and} \quad 0.1 \leq \alpha_2 \leq 2.0.$$

Based on the results of this simulation, the second stage have been performed, reducing the interval of the order of the integrators according to the region that has the lowest ISE criterion values and settling time. Therefore, for detailed analysis, several systems are simulated with variations of 0.01 within the ranges:

$$0.6 \leq \alpha_1 \leq 1.2 \quad \text{and} \quad 0.7 \leq \alpha_2 \leq 1.3.$$

The performance of this system is evaluated using the following criteria:

- Integral of the Squared Error (ISE) of the angular position of the pendulum:

$$J_\theta = \int_0^T \theta^2 dt$$

- Settling time of the pendulum  $t_\theta$ .
- Integral of the Squared Error (ISE) of the cart position:

$$J_x = \int_0^T x^2 dt$$

- Settling time of the cart  $t_x$ .

These criteria are imposed to verify the best combination of the orders  $\alpha_1$  and  $\alpha_2$ .

#### 4 Angular position of the pendulum

In the problem of an inverted cart-pendulum, the angular position of the pendulum is the most important output of the system for dynamic control, especially when the purpose of the control is to keep the pendulum in equilibrium in a near upright position. Therefore, the shorter the time and the oscillation for the system to reach this equilibrium, the better its performance. Therefore, during the simulations below, the setting time  $t_\theta$  and the ISE criterion  $J_\theta$  of the angular position are observed.

##### Global analysis

The first simulation to understand the behavior of the angular position varies  $\alpha_1$  and  $\alpha_2$  in the range 0.1 to 2. In this way, the ISE criterion for different combinations of integrators produce the results shown in Figures 3 and 4.

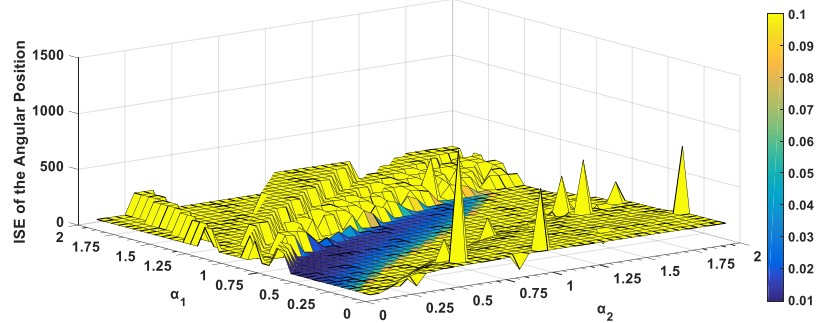
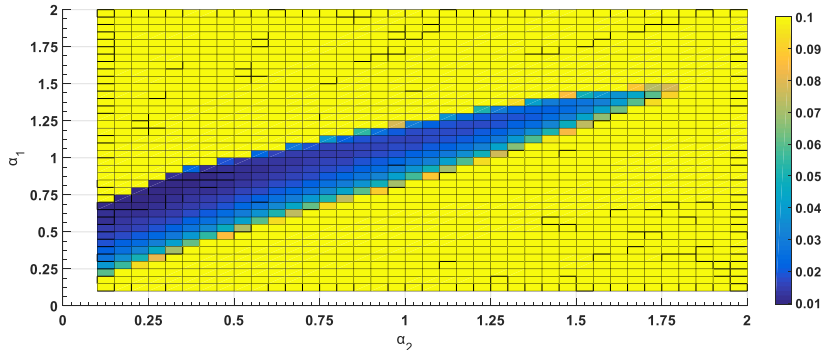


Figure 3: ISE criterion of the angular position for  $0.1 \leq \alpha_{1,2} \leq 2$ .



**Figure 4:** ISE criterion of the angular position for  $0.1 \leq \alpha_{1,2} \leq 2$ .

This first result already allows one to conclude that a system with low amplitudes and small oscillations (smaller  $J_\theta$ ) can be obtained through fractional integrators, as they present better results than integer integrators ( $\alpha_1 = \alpha_2 = 1$ ). Figure 4 shows the region of integrators that have the lowest ISE value in blue, reaching minimum values close to  $J_\theta=0.01$ .

Observing the results of another evaluation criterion, the numbers of combinations of integrators can be reduced, further detailing the analysis. Figures 5 and 6 show the results of the settling time of the first simulation.

Figure 5 shows regions with extremely low levels of settling time, however these regions have very oscillation values and high  $J_\theta$  values. Therefore, the point where the settling time and little oscillation is lower has been indicated in the graph.

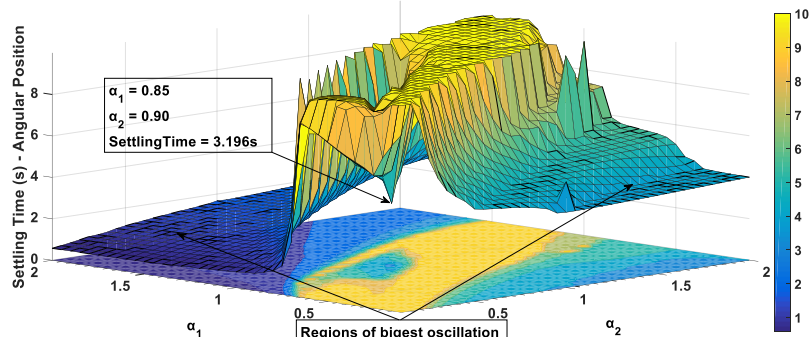


**Figure 5:** Settling time of the angular position for  $0.1 \leq \alpha_{1,2} \leq 2$ .

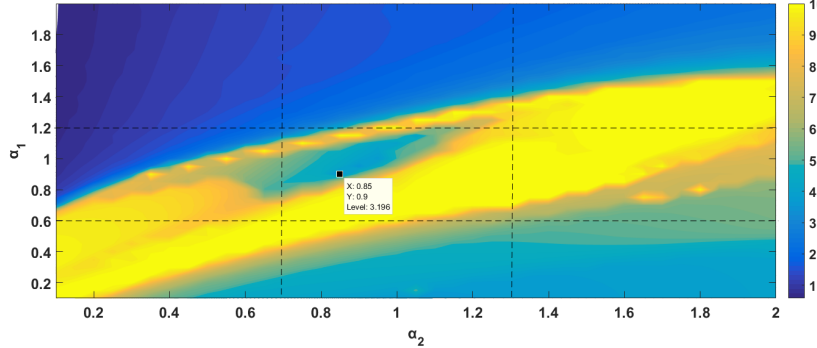


**Figure 6: Settling time of the angular position for  $0.1 \leq \alpha_{1,2} \leq 2$ .**

As in the results of the ISE criterion, the shortest settling time of the system does not correspond to the integers, but the combination of the fractional integrators  $\alpha_1 = 0.85$  and  $\alpha_2 = 0.90$ , as shown in Figure 5. These results also contribute to the details of the study, since it reduces the number of combinations of integrators with satisfactory results. If a controller with integer integrators ( $\alpha_{1,2} = 1$ ) has a settling time of 4.8 seconds, then the satisfactory results will be those below that. Therefore, for the next simulation the interval is reduced to:

$$0.6 \leq \alpha_1 \leq 1.2 \quad \text{and} \quad 0.7 \leq \alpha_2 \leq 1.3.$$

This range is represented by the central region of the settling time of the contour plot (Figure 6), bounded by dashed lines, where this minimum point and the other points satisfactory.

### Detailed analysis

In this second simulation, the intention is to find the minimum ISE criterion value of the angular position ( $J_\theta = \int_0^T \theta^2 dt$ ) together with the settling time  $t_\theta$  less than 4.8 seconds.

Thus, from the range defined in items 3.2 and 4.1.1, the ISE criteria and the settling time of the different combinations of integrators presented the results shown in Figures 7, 8, 9 and 10.

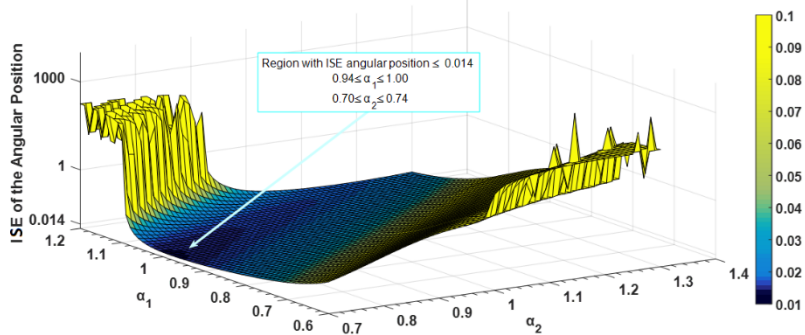


**Figure 7:** ISE criterion of the angular position for  $0.6 \leq \alpha_1 \leq 1.2$  and  $0.7 \leq \alpha_2 \leq 1.3$ .

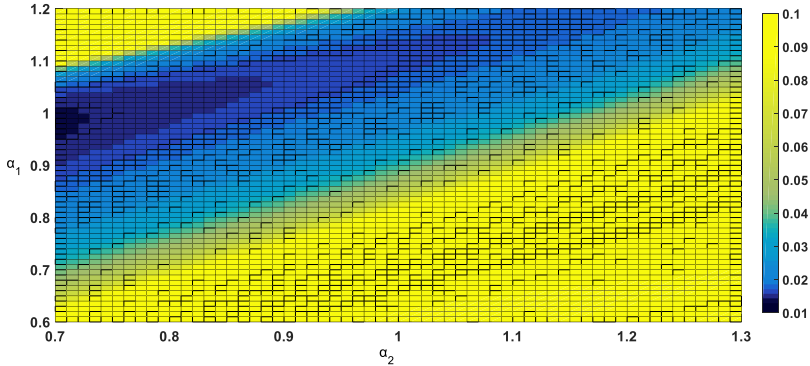


**Figure 8:** ISE criterion of the angular position for  $0.6 \leq \alpha_1 \leq 1.2$  and  $0.7 \leq \alpha_2 \leq 1.3$ .

The results of the graph in Figures 7 and 8 indicate to the minimum value of  $J_\theta$  equal to 0.014, with the fractional integrators approximately  $0.94 \leq \alpha_1 \leq 1.00$  and  $0.70 \leq \alpha_2 \leq 0.74$ , reaffirming that the use of fractional-order in the integrator is more advantageous.

As shown in Figure 9, the minimum settling time of the angular position is 2.315 and 3.182 seconds, with fractional integrators equal to  $\alpha_1 = 1.20 / \alpha_2 = 0.70$  and  $\alpha_1 = 0.86 / \alpha_2 = 0.90$ , respectively. However, the region around  $\alpha_1 = 1.20 / \alpha_2 = 0.70$  has high values of  $J_\theta$  (see figure 7). Figure 10 shows that there is a large region with different combinations of integrators with  $t_\theta$  below 4.8 seconds, even so for the two criteria these regions are different. Therefore, it is necessary to find an intersection of these criteria.

Therefore, to find the minimum value, the following optimization criterion is used

$$\text{Minimize } J_\theta = \int_0^T \theta^2 dt.$$

Imposing a settling time for the pendulum  $t_\theta \leq 4.8s$  and for the cart position  $t_x \leq 5s$ , the values obtained for the control system are  $\alpha_1 = 1.08$  and  $\alpha_2 = 0.95$ .

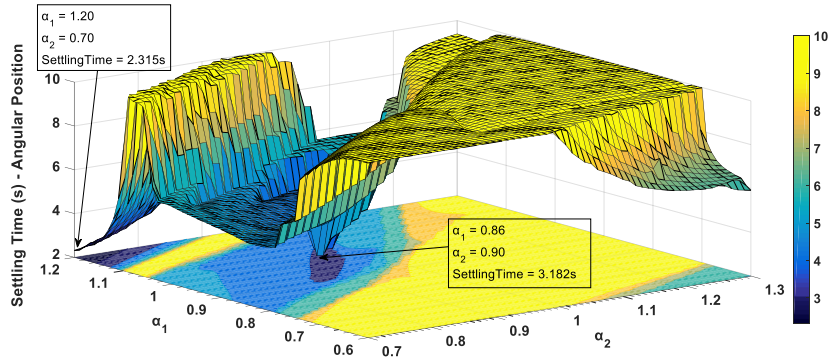


Figure 9: Settling time of the angular position for  $0.6 \leq \alpha_1 \leq 1.2$  and  $0.7 \leq \alpha_2 \leq 1.3$ .

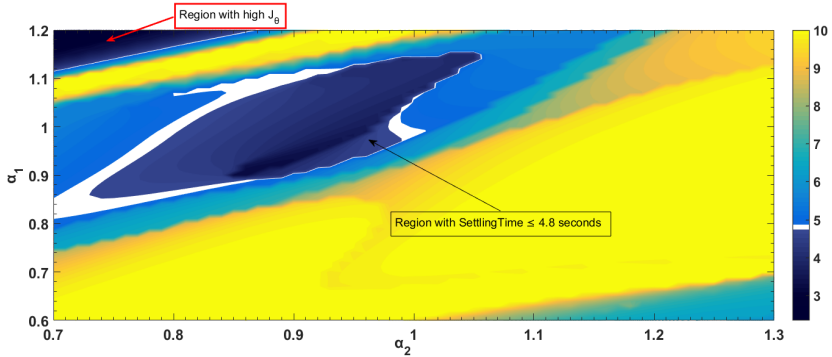


Figure 10: Settling time of the angular position for  $0.6 \leq \alpha_1 \leq 1.2$  and  $0.7 \leq \alpha_2 \leq 1.3$ .

## 5 Position of the cart

The dynamic control of the cart's position output is important when the system's objective is to reduce the cart's travel as much as possible while maintaining the pendulum in equilibrium in the vertical position, i.e. the final angle  $\theta_f$  near zero. Therefore, the shorter the settling time for the system to reach this equilibrium with lower amplitudes and oscillations, the better its performance. Therefore, during the simulations below, the settling time  $t_x$  and the ISE criterion  $J_x$  of the cart position are observed.

### Global analysis

The simulation is performed to comprehend the behavior of the cart position in a global way, varying  $\alpha_1$  and  $\alpha_2$  in the range of 0.1 to 2. Thus, the ISE criterion of the different combinations of integrators presented the results shown in Figure 11 and 12.

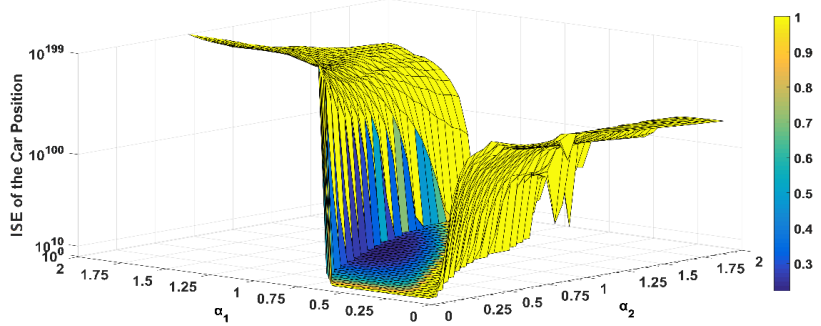


Figure 11: ISE criterion of the cart position  $0.1 \leq \alpha_{1,2} \leq 2$ .

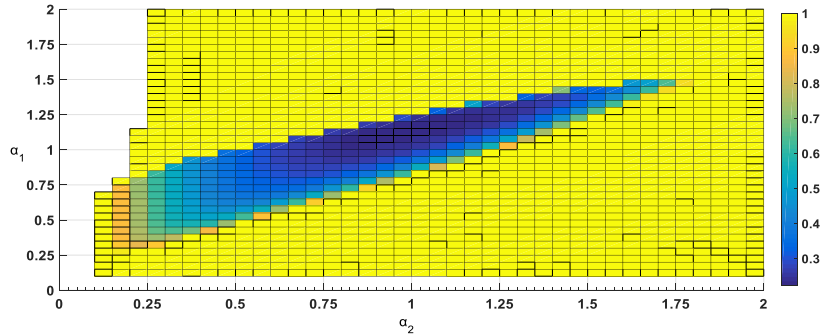
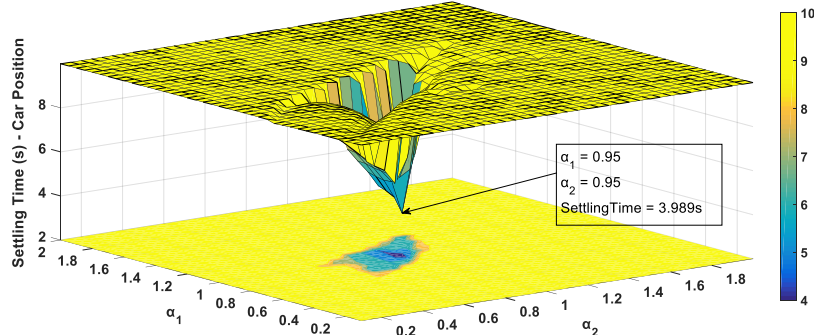
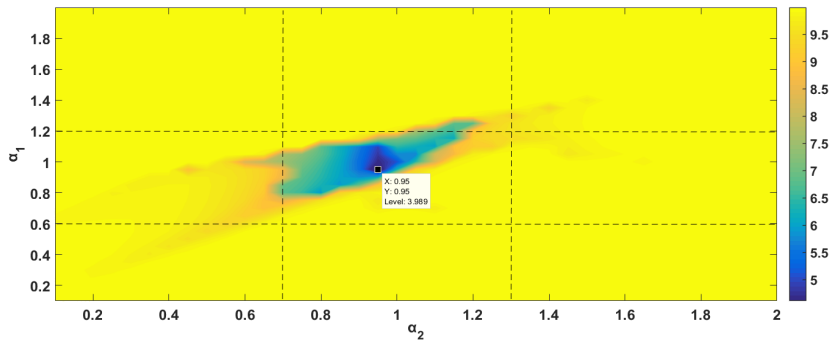


Figure 12: ISE criterion of the cart position for  $0.1 \leq \alpha_{1,2} \leq 2$ .



**Figure 13:** Settling time of the cart position for  $0.1 \leq \alpha_{1,2} \leq 2$ .



**Figure 14:** Settling time of the cart position for  $0.1 \leq \alpha_{1,2} \leq 2$ .

To reduce the number of combinations of integrators and to further detailed analysis, the results of settling time are observed, as shown in Figures 13 and 14.

Figures 13 and 14 shows that the shortest settling time in the system does not correspond to the integer integrators, but the combination of the fractional integrators  $\alpha_1 = 0.95$  and  $\alpha_2 = 0.95$ , with settling time equal to 4.0 seconds. These results also contribute to the details of the study, since it reduces the number of combinations of integrators with satisfactory results. If a controller with integer integrators ( $\alpha_{1,2} = 1$ ) has a settling time of the cart position equal to 5.0 seconds, then the satisfactory results are be those below that. Therefore, the same simulation of the detailed analysis of the angular position is conducted with intervals equal to:

$$0.6 \leq \alpha_1 \leq 1.2 \quad \text{and} \quad 0.7 \leq \alpha_2 \leq 1.3.$$

This range is represented by the central region of the settling time of the contour plot (Figure 14), bounded by dashed lines, where this minimum point and the other points satisfactory.

### Detailed analysis

In the detailed analysis the objective is to find the minimum ISE criterion value of the cart position ( $J_x = \int_0^T x^2 dt$ ) together with the  $t_x$  settling time less than 5 seconds. Thus, from the interval defined in items 3.2 and 4.2.1, the ISE criterion and the settling time of the different combinations of integrators presented the results shown in Figures 15, 16, 17 and 18.

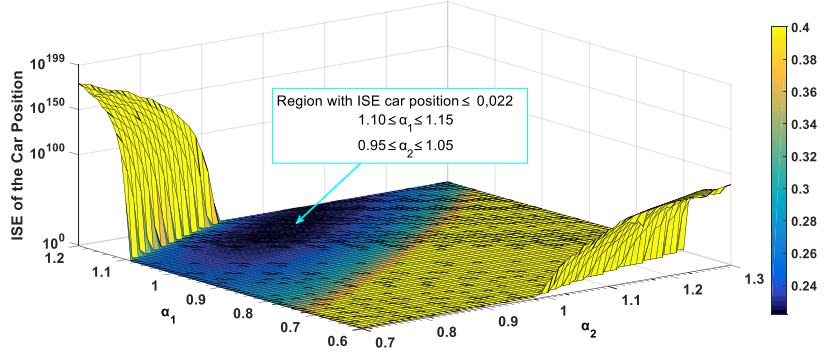


**Figure 15:** ISE criterion of the cart position for  $0.6 \leq \alpha_1 \leq 1.2$  and  $0.7 \leq \alpha_2 \leq 1.3$ .

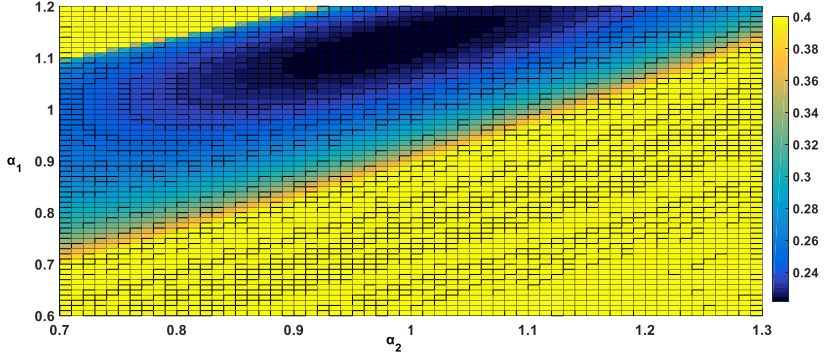


**Figure 16:** ISE criterion of the cart position for  $0.6 \leq \alpha_1 \leq 1.2$  and  $0.7 \leq \alpha_2 \leq 1.3$ .

The results of the graph in Figures 15 and 16 indicate to the minimum value of  $J_x$  equal to 0.22, with the fractional integrators approximately  $1.10 \leq \alpha_1 \leq 1.15$  and  $0.95 \leq \alpha_2 \leq 1.05$ , again reaffirming that the use of fractional-order in the integrator offers better results.

As shown in Figures 17, the minimum settling time of the angular position is 3.72 seconds, with fractional integrators equal to  $\alpha_1 = 0.95$  and  $\alpha_2 = 0.97$ . Figure 18 shows that there is a small region with different combinations of integrators with  $t_x$  below 5 seconds, even so for the two criteria these regions are different. Therefore, it is necessary to find an intersection of these criteria.

Therefore, to find the minimum value, the following optimization criterion is used

$$\text{Minimize } J_x = \int_0^T x^2 dt.$$

Imposing a settling time for the pendulum  $t_\theta \leq 4.5s$  and for the cart position  $t_x \leq 5s$ , the values obtained for the control system are also  $\alpha_1 = 1.10$  and  $\alpha_2 = 0.95$ .

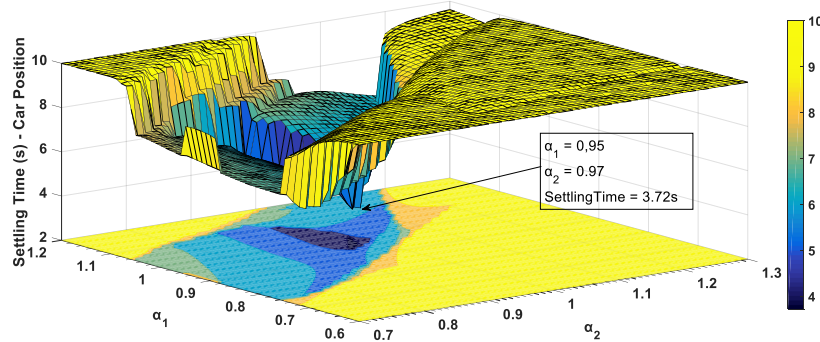


**Figure 17:** Settling time of the car position for  $0.6 \leq \alpha_1 \leq 1.2$  and  $0.7 \leq \alpha_2 \leq 1.3$ .

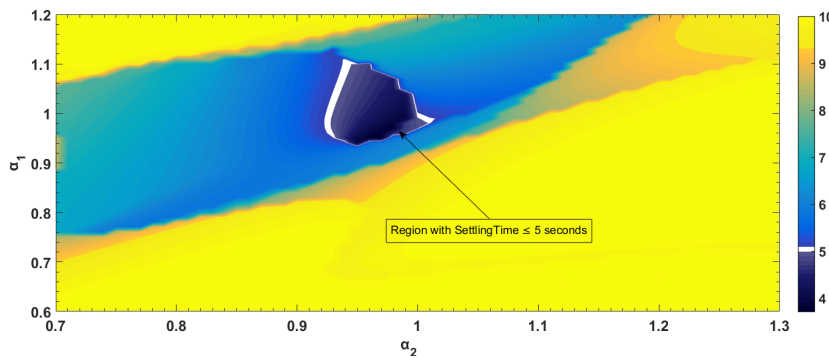


**Figure 18:** Settling time of the cart position for  $0.6 \leq \alpha_1 \leq 1.2$  and  $0.7 \leq \alpha_2 \leq 1.3$ .

## 6 Optimized controller

The previous items indicate that for both, the control of the angular position and the control of the position of the cart, the ideal value for the order of the integrators is equal to  $\alpha_1 = 1.08/1,10$  and  $\alpha_2 = 0.95$ . Thus, it is concluded that the fractionals result in a better performance. Otherwise, the optimization should have indicated the order of the integrators equal to 1.

To reinforce the advantages of fractional controllers, graphical and performance comparisons are made, based on the criteria: settling time and ISE criteria. The fractional integrators  $\alpha_1 = 1.09$  (middle term between the optimization of  $J_\theta$  and  $J_x$ ) and  $\alpha_2 = 0.95$  were used. The graphical comparisons of system responses are shown in Figure 19 and Figure 20.

The graphs with the comparison between the control systems with integer and fractional integrators show better performance in both criteria. The values of the performance criteria of both systems are presented in the Table 1.

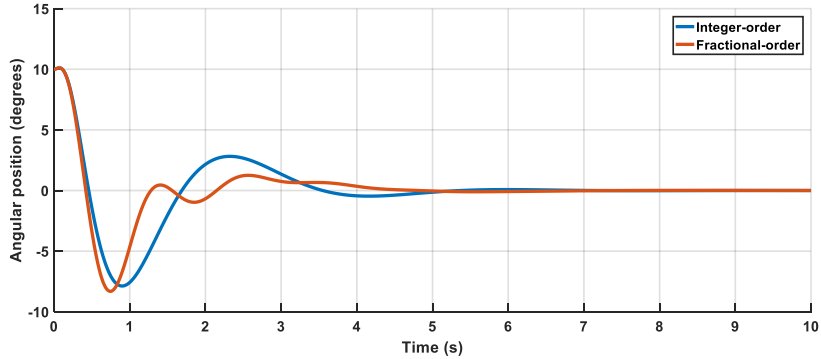


Figure 19: Time series of the angular position of the pendulum when ISE criteria is minimized imposing  $t_\theta \leq 4.8s$  and  $t_x \leq 5s$ .

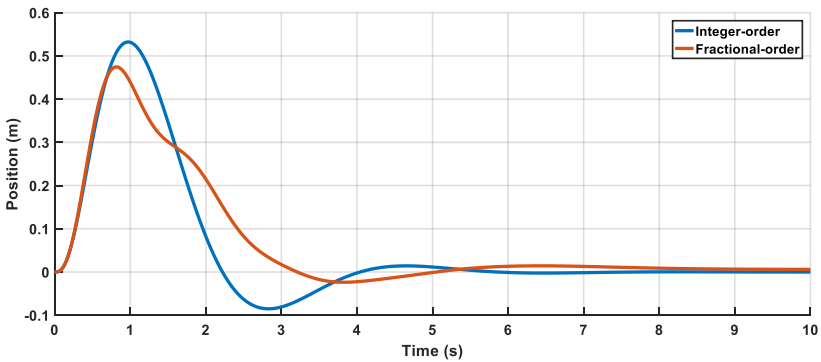


Figure 20: Time series of the position of the cart when ISE criteria is minimized imposing  $t_\theta \leq 4.8s$  and  $t_x \leq 5s$ .

**Table 1 - Performance values of systems with integer and fractional integrators after optimization of the ISE criterion of the angular position**

Parameter	ISE			Settling Time		
	IO	FO	%	IO	FO	%
Angular position	68.63	53.04	-23	4.87	4.19	-14
Cart position	0.26	0.22	-14	5.07	4.91	-3

The results in Table 1 refer to the optimization of the ISE criterion with the settling time, where the ISE angular position presenting the best performance among the other criteria (approximately 23%). There is also an improvement of the 14% in the ISE criteria of the cart position and the settling time of the angular position. The only one that does not have a considerable improvement is the settling time of the cart position. However, it is concluded that there is a possibility of improving the controllers using fractional integrators.

The ideal order values found can be different according to the priority that is given to the dynamic control of the system, that is, if the objective is to improve the settling time of the cart independent of the settling time pendulum, the order of the integrators will be different of the optimum found.

## 7 Basins of attraction

### Optimized controller ( $\alpha_1 = 1$ and $\alpha_2 = 0.95$ )

The basins of the attraction of the system are compared with integer and fractional integrators. Figure 21 show the result of the attraction basins in terms of angular position and angular velocity. For the fractional controller,  $\alpha_1 = 1.09$  and  $\alpha_2 = 0.95$  are considered.

The graph shown in Figures 21 show that the use of fractional-order integrators reduces the basin of attraction, despite improving performance. With the integer-order the angular position of the attraction basin is close to 50 degrees, while the fractional-order is below 40 degrees. The reduction in the number of controllable cases with different initial conditions using the fractional-order was 36% compared to the integer-order.

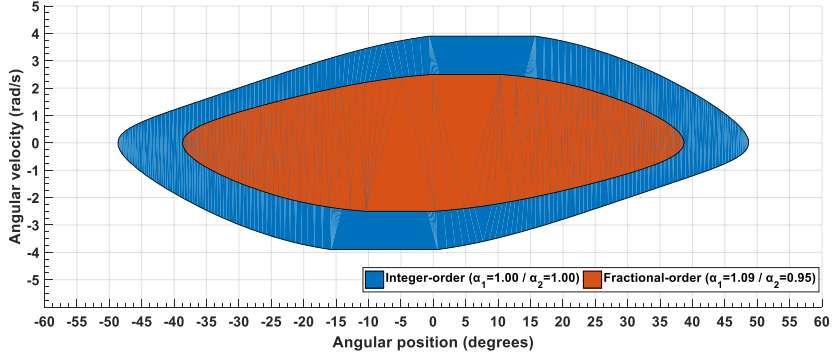


**Figure 21: Basin of attraction in the angular position vs angular velocity plane for the integrator with integer-order ( $\alpha_1 = 1$  and  $\alpha_2 = 1$ ) and fractional-order ( $\alpha_1 = 1.09$  and  $\alpha_2 = 0.95$ ).**

#### Controller with wider attraction basin ( $\alpha_1 = 0.90$ and $\alpha_2 = 0.85$ )

From the previous results, where the basin of attraction was reduced using an optimal controller, seek to find combinations of fractional orders that resulted in the opposite, i.e. an extension of the attraction basin. Therefore, the fractional integrators  $\alpha_1 = 0.90$  and  $\alpha_2 = 0.85$  are used and Figure 22 shows the attraction basins of the three cases (integer-order, optimal fractional-order and fractional-order with a wider attraction basin).

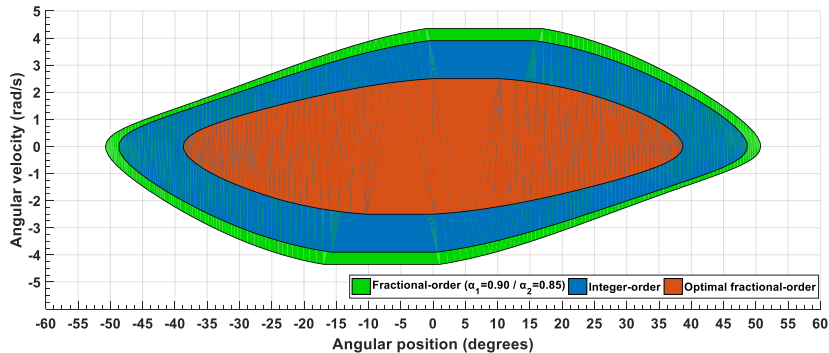


**Figure 22: Basins of attraction in the angular position vs angular velocity plane for the three cases of the integrators: integer-order, optimal fractional-order and fractional-order with a wider attraction basin.**

The basin of attraction of the new integrator with fractional orders  $\alpha_1 = 0.90$  and  $\alpha_2 = 0.85$  had an increase of 11% compared to the whole order integrator basin. Thus, it can be said that the use of fractional orders reduces and enlarges the attraction basin, being related to the combination of orders used. In addition,

this reduction or expansion is also related to the performance of the controller (settling time and ISE criteria). To assess the impact on the system's behavior, performance and graphical comparisons were made. The graphical comparisons of system responses are shown in Figure 23 and Figure 24.

The graphs show that performance is impaired, with fractional order resulting in higher amplitudes. For a better analysis, the settling time and the ISE criteria are shown in Table 2.

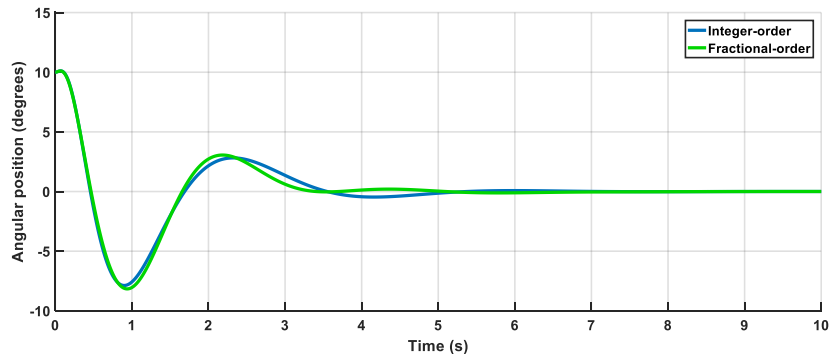


**Figure 23:** Comparison of time series of the angular position of the pendulum between integer-order and fractional-order with wider attraction basins.

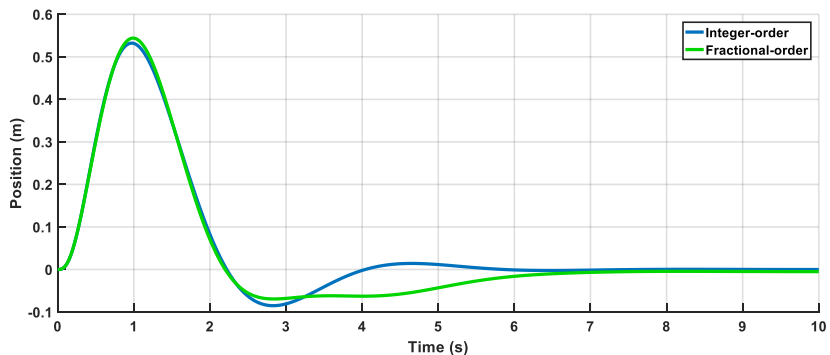


**Figure 24:** Comparison of time series of the position of the cart between integer-order and fractional-order with wider attraction basins.

Among the results of the criteria presented in Table 2, only the setting time of the angular position of the pendulum has the best performance in comparison with the integer-order controller, with a time reduction of 34%, even better than the optimal controller. The most significant worsening in performance was in the settling time of the cart position, with an increase in time of 18%. The other criteria had no significant variations.

**Table 2 - Performance values of systems with integer and fractional integrators with wider attraction basins.**

<b>Parameter</b>	<b>ISE</b>			<b>Settling Time</b>		
	<b>IO</b>	<b>FO</b>	<b>%</b>	<b>IO</b>	<b>FO</b>	<b>%</b>
Angular position	68.63	70.70	+3	4.87	3.20	-34
Cart position	0.26	0.27	+4	5.07	6.00	+18

## 8 Conclusions

Based on the results shown in this chapter, it can be concluded that the using of fractional integrators improves the performance of the control of a cart-pendulum system reducing the ISE of both the angular position and the position of the cart and the settling time either for the same combinations of  $k_i$ , but, as expected, the basin of attraction is reduced.

However, disregarding some performance criteria, fractional integrators can expand the attraction basin and improve a certain performance criterion at the same time, as shown in Table 2, where even with the 11% increase in the attraction basin, there is an 34% reduction in settling time compared to integer-order integrators.

The proposed approach seems to be very appealing for control systems in which state-derivatives are easier to be obtained or measured than the state signals (Assunção et al. 2007).

## Acknowledgments

The authors are grateful for the financial support received from the Brazilian agencies CAPES, CNPq and FAPERJ.

## References

- Monje, C. A., Chen, Y., Vinagre, B. M., Xue, D., & Feliu-Batle, V. (2010). Fractional-order systems and controls: fundamentals and applications. Springer Science & Business Media.
- Ortigueira, Manuel Duarte (2011). Fractional calculus for scientists and engineers. Springer Science & Business Media.
- Ortigueira, Manuel D.; Machado, JA Tenreiro. (2015) What is a fractional derivative? Journal of computational Physics, v. 293, p. 4-13
- C. Li and W. Deng (2007). Remarks on fractional derivatives. Applied Mathematics and Computation, 187:777–784.

- Caputo, Michele; Fabrizio, Mauro (2015). A new definition of fractional derivative without singular kernel. *Progr. Fract. Differ. Appl.*, v. 1, n. 2, p. 1-13.
- Khalil, Roshdi et al (2014). A new definition of fractional derivative. *Journal of Computational and Applied Mathematics*, v. 264, p. 65-70.
- Zheng, Zhibao; Zhao, Wei; DAI, Hongzhe (2019). A new definition of fractional derivative. *International Journal of Non-Linear Mechanics*, v. 108, p. 1-6.
- Ortigueira, Manuel D.; Trujillo, Juan J (2012). A unified approach to fractional derivatives. *Communications in Nonlinear Science and Numerical Simulation*, v. 17, n. 12, p. 5151-5157.
- Katugampola, Udita N (2011). New approach to a generalized fractional integral. *Applied Mathematics and Computation*, v. 218, n. 3, p. 860-865.
- Li, Changpin; Chen, An; Ye, Junjie (2011). Numerical approaches to fractional calculus and fractional ordinary differential equation. *Journal of Computational Physics*, v. 230, n. 9, p. 3352-3368.
- Deng, Jingwei; Zhao, Lijing; Wu, Yujiang (2015). Efficient algorithms for solving the fractional ordinary differential equations. *Applied Mathematics and Computation*, v. 269, p. 196-216.
- Teplyakov, Aleksei; Petlenkov, Eduard; Belikov, Juri (2011). FOMCOM: a MATLAB toolbox for fractional-order system identification and control. *International Journal of Microelectronics and computer science*, v. 2, n. 2, p. 51-62.
- Katsikadelis, John T (2015). Generalized fractional derivatives and their applications to mechanical systems. *Archive of Applied Mechanics*, v. 85, n. 9-10, p. 1307-1320.
- Caputo, Michele; Carcione, José M (2011). Hysteresis cycles and fatigue criteria using anelastic models based on fractional derivatives. *Rheologica acta*, v. 50, n. 2, p. 107-115.
- Lewandowski, Roman; Pawlak, Zdzisław (2018). Response spectrum method for building structures with viscoelastic dampers described by fractional derivatives. *Engineering Structures*, v. 171, p. 1017-1026.
- Lin, R. M.; Ng, T. Y (2019). Eigenvalue and eigenvector derivatives of fractional vibration systems. *Mechanical Systems and Signal Processing*, v. 127, p. 423-440.
- Dai, Hongzhe; Zheng, Zhibao; Wang, Wei (2017). On generalized fractional vibration equation. *Chaos, Solitons & Fractals*, v. 95, p. 48-51.
- Teplyakov, Aleksei (2017). Fractional-order modeling and control of dynamic systems. Springer.
- Shah, P. and Agashe, S. (2016). Review of fractional PID controller. *Mechatronics*, 38:29-41.
- Chen, Kai et al (2018). Fractional-order PI $\lambda$  controller synthesis for steam turbine speed governing systems. *ISA transactions*, v. 77, p. 49-57.
- Bingul, Zafer; Karahan, Oguzhan (2018). Comparison of PID and FOPID controllers tuned by PSO and ABC algorithms for unstable and integrating systems with time delay. *Optimal Control Applications and Methods*, v. 39, n. 4, p. 1431-1450.
- Li, Dazi; Ding, Pan; GAO, Zhiqiang (2016). Fractional active disturbance rejection control. *ISA transactions*, v. 62, p. 109-119.
- Balachandran, Krishnan et al (2015). Controllability of fractional damped dynamical systems. *Applied Mathematics and Computation*, v. 257, p. 66-73.
- Barbosa, Ramiro S.; Machado, Ja Tenreiro; Jesus, Isabel S (2010). Effect of fractional-orders in the velocity control of a servo system. *Computers & Mathematics with Applications*, v. 59, n. 5, p. 1679-1686.
- Wang, Z. H.; Zheng, Y. G (2009). The optimal form of the fractional-order difference feedbacks in enhancing the stability of a sdof vibration system. *Journal of Sound and Vibration*, v. 326, n. 3-5, p. 476-488.

- Xue, Ding-Y; Zhao, Chun-Na (2007). Fractional-order PID controller design for fractional-order system. *Control Theory & Applications*, v. 5, p. 771-776.
- Delavari, H. et al (2010). Fractional-order control of a coupled tank. *Nonlinear Dynamics*, v. 61, n. 3, p. 383-397.
- Martelli, Gianpasquale (2009). Stability of PID-controlled second-order time-delay feedback systems. *Automatica*, v. 45, n. 11, p. 2718-2722.
- Azar, Ahmad Taher; Vaidyanathan, Sundarapandian; Ouannas, Adel (2017). Fractional-order control and synchronization of chaotic systems. Springer.
- Niu, Jiangchuan et al (2017). Analysis of Duffing oscillator with time-delayed fractional-order PID controller. *International Journal of Non-Linear Mechanics*, v. 92, p. 66-75.
- Shen, Yong-Jun; Yang, Shao-Pu; Sui, Chuanyi (2014). Analysis on limit cycle of fractional-order van der Pol oscillator. *Chaos, Solitons & Fractals*, v. 67, p. 94-102.
- Shen, Yong-Jun; Wei, Peng; Yang, Shao-Pu (2014). Primary resonance of fractional-order van der Pol oscillator. *Nonlinear Dynamics*, v. 77, n. 4, p. 1629-1642.
- Kharola, Ashwani et al (2016). A comparison study for control and stabilisation of inverted pendulum on inclined surface (IPIS) using PID and fuzzy controllers. *Perspectives in Science*, v. 8, p. 187-190.
- Wang, Ling et al (2014). MBPOA-based LQR controller and its application to the double-parallel inverted pendulum system. *Engineering Applications of Artificial Intelligence*, v. 36, p. 262-268.
- Prasad, Lal Bahadur; Tyagi, Barjeev; Gupta, Hari Om (2014). Optimal control of nonlinear inverted pendulum system using PID controller and LQR: performance analysis without and with disturbance input. *International Journal of Automation and Computing*, v. 11, n. 6, p. 661-670.
- Wang, Jia-Jun (2011). Simulation studies of inverted pendulum based on PID controllers. *Simulation Modelling Practice and Theory*, v. 19, n. 1, p. 440-449.
- Mousa, M. E.; Ebrahim, Mohamed A.; Hassan, Ma Moustafa (2017). Optimal fractional-order proportional—integral—differential controller for inverted pendulum with reduced order linear quadratic regulator. In: *Fractional-order Control and Synchronization of Chaotic Systems*. Springer, Cham, p. 225-252.
- Assunção, E.; Teixeira, M. C. M.; Faria, F. A., Da Silva, N. A. P., & Cardim (2007), R. Robust state-derivative feedback LMI-based designs for multivariable linear systems. *International Journal of Control*. V.80, P. 1260-1270.